

Bioinformatic Analysis Revealing Mitotic Spindle Assembly regulated NDC80 and MAD2L1 as Prognostic Biomarkers in Non-Small Cell Lung Cancer Development

Rong Wei

The Second Hospital of ShanXi Medical University

Ziyue Wang

The Second Hospital of ShanXi Medical University

Yaping Zhang

The Second Hospital of ShanXi Medical University

Bin Wang

The Second Hospital of ShanXi Medical University

Ningning Shen

The Second Hospital of ShanXi Medical University

Li E

The Second Hospital of ShanXi Medical University

Xin Li

The Second Hospital of ShanXi Medical University

Lifang Shang

The Second Hospital of ShanXi Medical University

Yangwei Shang

The Second Hospital of ShanXi Medical University

Wenpeng Yan

The Second Hospital of ShanXi Medical University

Xiaoqin Zhang

The Second Hospital of ShanXi Medical University

Wenxia Ma

The Second Hospital of ShanXi Medical University

Chen Wang (✉ wangchen8877322@126.com)

The Second Hospital of ShanXi Medical University <https://orcid.org/0000-0002-4919-9677>

Research article

Keywords: non-small cell lung cancer (NSCLC), lung adenocarcinoma (LUAD), squamous cell carcinoma (LUSC), GEO database, TCGA data, biomarker

Posted Date: August 6th, 2020

DOI: <https://doi.org/10.21203/rs.3.rs-43770/v3>

License: © ⓘ This work is licensed under a Creative Commons Attribution 4.0 International License. [Read Full License](#)

Version of Record: A version of this preprint was published on August 14th, 2020. See the published version at <https://doi.org/10.1186/s12920-020-00762-5>.

Abstract

Background Lung cancer has been the leading cause of tumor related death, and 80%~85% of it is non-small cell lung cancer (NSCLC). Even with the rising molecular targeted therapies, for example EGFR, ROS1 and ALK, the treatment is still challenging. The study is to identify credible responsible genes during the development of NSCLC using bioinformatic analysis, developing new prognostic biomarkers and potential gene targets to the disease.

Methods Firstly, three genes expression profiles GSE44077, GSE18842 and GSE33532 were picked from Gene Expression Omnibus (GEO) to analyze the genes with different expression level (GDEs) between NSCLC and normal lung samples, and the cellular location, molecular function and the biology pathways the GDEs enriched in were analyzed. Then, gene function modules of GDEs were explored based on the protein-protein interaction network (PPI), and the top module which contains most genes was identified, followed by containing genes annotation and survival analysis. Moreover, multivariate cox regression analysis was performed in addition to the Kaplan meier survival to narrow down the key genes scale. Further, the clinical pathological features of the picked key genes were explored using TCGA data.

Results Three GEO profiles shared a total of 664 GDEs, including 232 up-regulated and 432 down-regulated genes. Based on the GDEs PPI network, the top function module containing a total of 69 genes was identified, and 31 of 69 genes were mitotic cell cycle regulation related. And survival analysis of the 31 genes revealed that 17/31 genes statistical significantly related to NSCLC overall survival, including 4 spindle assembly checkpoints, namely NDC80, BUB1B, MAD2L1 and AURKA. Further, multivariate cox regression analysis identified NDC80 and MAD2L1 as independent prognostic indicators in lung adenocarcinoma (LUAD) and squamous cell carcinoma (LUSC) respectively. Interestingly, pearson correlation analysis indicated strong connection between the four genes NDC80, BUB1B, MAD2L1 and AURKA, and their clinical pathological features were addressed.

Conclusions Using bioinformatic analysis of GEO combined with TCGA data, we revealed two independent prognostic indicators in LUAD and LUSC respectively and analyzed their clinical features. However, more detailed experiments and clinical trials are needed to verify their drug targets role in clinical medical use.

Background

Lung cancer has been a common malignant tumor worldwide¹, with the morbidity only second to prostatic cancer in male and breast cancer in female². As for the mortality, lung cancer has been the top killer of cancer-related death both in male and female for decades^{3,4}. The other two cancer-related death that next to lung cancer are prostatic cancer and colorectal cancer in male, as well as breast cancer and colorectal cancer in female, the four cancer types taking up 45% of the whole malignant tumor related death roll. Meanwhile within the lung cancer, 80%~85% is non-small cell lung cancer (NSCLC), including adenocarcinoma, squamous cell carcinoma and large cell carcinoma.²

Besides the traditional surgery, chemotherapy and radiotherapy, targeted therapy is a newly developed clinical curative method in NSCLC involving tens genes, including EGFR, ALK, ROS1, BRAF, HER2, PIK3CA, RET and so on⁵. For instance, the discovery of the frequent mutation of EGFR in NSCLC especially lung adenocarcinoma in non-smoking female Asia patients leading to the development of generations EGFR-TKI (tyrosine kinase inhibitors) treatment, which has been showing effective results⁶⁻⁸. Additionally, the rearrangements of ALK, ROS1 and RET genes bring in the development of therapeutic TKI treatments, for instance crizotinib and lorlatinib^{9,10}. The overall disease responsive rate is reported to be as high as 55%, meanwhile the progression-free survival rate reaches 72% in NSCLC patients with ALK rearrangement.^{11,12}

However, the currently available drug targets are lacking as opposed to the progressively developing cancer. Even with the rising molecular targeted therapies that shows promising treatment effects, the current situation for NSCLC clinical treatment is not promising. To understand more clear about the genetic information of NSCLC thus identifying potential prognostic biomarkers and new drug targeting genes is of great importance.

Recently, the development of high-throughput technologies, for instance protein chips, next generation sequencing and single cell sequencing bring in tremendous molecular data, which are publicly available, providing great chances for us to uncover novel genomic targets for therapeutic intervention^{13,14}.

In the study, three cDNA expression profiles GSE44077¹⁵, GSE18842¹⁶ and GSE33532¹⁷ were firstly picked from Gene Expression Omnibus(GEO) based on their sample number to detect the genes with different expression level (GDEs) in NSCLC versus normal lung samples. Then, based on the protein-protein interacting (PPI) network of GDEs, GDEs function modules were analyzed and the top module containing most GDEs was picked, and all the containing genes were identified to evaluate the association with patients overall survival (OS) using KM plot online database and cox regression analysis. Moreover, the cellular component, molecular functions, signaling pathways and biological processes of the hub genes, namely the genes that were statistical significantly correlate with NSCLC OS would be analyzed, and their clinical pathological features would be evaluated using TCGA data. The results shall be useful for identifying new prognostic biomarkers and potential gene targets in clinical NSCLC treatment.

Methods

Data source: three cDNA profiles from GEO online database

From GEO online public database¹⁸, three cDNA expression datasets GSE18842, GSE44077 and GSE33532 were picked based on the sample size (Only the profiles that contain at least 20 paired samples were considered). Within the 3 profiles, GSE18842 was based on GPL570[HG-U133_Plus_2] Affymetrix Human Genome U133 Plus 2.0 Array, containing 46 NSCLC cancer and 45 normal lung samples. And GSE44077 profile was based on GPL6244[HuGene-1_0-st] Affymetrix Human Gene 1.0 ST Array, including 55 cancer and 66 normal lung samples. And GSE33532 was based on GPL570[HG-U133_Plus_2] Affymetrix Human Genome U133 Plus 2.0 Array, covering 80 cancer and 20 normal samples.

Unearth of the GDEs in NSCLC from normal lung samples

GEO2R tool¹⁹ is provided paired with GEO data online, and in the study, it was used to analyze the GDEs between NSCLC and normal lung samples. The criteria for GDEs identification were set as $|\log_2FC| \geq 1$ and adjusted P value < 0.05 .

Pathway enrichment of GDEs revealed by GO and KEGG

Gene ontology analysis (GO) is effectively used to identify characteristic biological attributes of high-throughput genetic data. Meanwhile Kyoto Encyclopedia of Genes and Genomes (KEGG) is a collection of high throughput biological information covering genomes, cells, signaling pathways and so on, it is commonly used for annotation the lists of genes and interpretation of the network of signaling pathways involved. GO and KEGG analysis were performed using FUNRICH3.1 software²⁰ to reveal the functions enrichment of the GDEs shared in three GEO profiles, including their cellular components, molecular functions, biological processes and the signaling pathways they mainly enriched in.

Construction of the PPI network of GDEs

STRING²¹ is short for Search Tool for the Retrieval of interacting Genes, and it was used in the study to analyze the protein-protein interaction(PPI) of the GDEs uncovered by GEO2R. The analyzing criteria was set as confidence score ≥ 0.4 and maximum interactors number =0.

GDEs function module analysis based on PPI network

Molecular Complex Detection (MCODE) plug-in of Cytoscape3.6.0 software²² was used to screen gene function modules based on GDEs PPI network, with the degree cut-off set as 2, node score cut off set as 0.2, the k-core equals 2, and max depth equals 100. Using MCODE analysis, we identified the top gene module (gene clusters sharing similar function)

containing most GDEs, and GO and KEGG were further performed to annotate the genes and explore the signaling pathways of the gene modules.

Survival analysis of module genes to identify key genes

Kaplan Meier plot²³ is an openly accessed online service for analyzing univariate overall survival correlation of multiple genes in various cancers including lung cancer. In the study, Kaplan Meier plot was firstly used to analyze the OS prognosis information of all the genes in the top module to screen for the genes that have statistical significant correlation with NSCLC patients survival.

And then multivariate COX regression analysis was performed using TCGA mRNA transcription data including 223 lung adenocarcinoma and 482 lung squamous cell carcinoma, which were downloaded from TCGA database²⁴ to identify the independent prognostic indicators from the univariate significant gene lists. Further, the genes' association with clinical features were validated using lung adenocarcinoma and lung squamous cell carcinoma samples data provided on an online server UALCAN.

Related signaling pathways and co-expression genes analysis

GEPIA²⁵ is a commonly used online service for analyzing certain genes expression differences between cancer and normal tissues in various tumor types and exploring the correlation between genes. In the study, we used GEPIA to analyze key genes' (the genes that statistical significantly correlates with NSCLC OS) general expression in lung cancer comparing to normal lung samples and explore the genes that harbor similar expression with analyzed key genes.

Results

Identification of 664 GDEs shared by three GEO profiles

Three GEO cDNA profiles GSE44077, GSE18842 and GSE33532 were picked to analyze the GDEs in cancer vs. normal lung samples. And a whole of 1133, 4459 and 3775 GDEs including 691, 2505, 2351 down-regulated and 442, 1954, 1424 up-regulated genes were identified in GSE44077 (Figure 1A), GSE18842 (Figure 1B) and GSE33532 (Figure 1C) respectively. Additionally, 432 down-regulated and 232 up-regulated GDEs were shared among the three GEO profiles showed by Venn diagram performance (Figure 1D, 1E).

Pathway enrichment analysis of shared GDEs by GO and KEGG

To further understand the pathways 664 GDEs were mainly enriched in, GO and KEGG analysis were conducted. Interestingly, GO analysis showed that the cell components of 232 up-regulated GDEs were enriched in centrosome, microtubule and kinetochore (Figure 2A), and the molecular function were focused on metalloproteinase activity (Figure 2B). The biological process were mostly enriched in cell growth and maintenance, spindle assembly and chromosome segregation (Figure 2C). Moreover, KEGG/biological pathway analysis showed the up-regulated GDEs were mostly involved in cell mitotic and DNA replication (Figure 2D). Three of the four aspects including genes cell component, signaling pathways and biological process suggested the orientation of cell cycle mitotic process, indicating the potential value of cell division process in cancer targeting treatment.

Meanwhile, as for the 432 down regulated GDEs, the cell components were primary focused on cellular plasma membrane (Figure 2E), the molecular function were enriched in receptor activity and cell adhesion molecular activity (Figure 2F), and the biological process were mainly enriched in signal transduction and cell communication (Figure 2G). Additionally, KEGG/biological pathway analysis showed the down-regulated GDEs were mostly participated in hemostasis, cell surface interaction at vascular walls and Epithelial to Mesenchymal transition (EMT) (Figure 2H).

Function module analysis based on PPI network

To identify the potential responsible genes in NSCLC development, the PPI network of 664 GDEs was constructed with STRING, and the function modules of the GDEs were analyzed. Based on the PPI, top three gene modules were identified containing 69, 27 and 28 genes respectively (Figure 3A), and these three modules were named as Gene Cluster1 (Figure 3D), 2 (Figure 3B) and 3 (Figure 3C) accordingly.

GO and KEGG result revealed that most of the Cluster 1 genes were enriched in the cell cycle (31/69), DNA replication (22/69) and Mitotic M-M/G1 (20/69) related signaling (Figure 3E). All the signaling that Cluster1 genes enriched in were sorted in descending order based on the gene counts and FDR value (Table 1). We primarily focused on the top cell cycle regulation related module which matches most GDEs in the network, and we further perform survival analysis on all the 31 genes.

Survival analysis of Cluster 1 module genes

Univariate Kaplan Meier plot overall survival analysis of 31 cell cycle regulation genes in Gene Cluster 1 showed that 17 out of 31 genes statistical significantly correlates with patients overall survival, including 4 spindle assembly checkpoints BUB1 (Figure4A), NDC80 (Figure4C), MAD2L1 (Figure4E), and AURKA (Figure4G). And GEPIA was then used to validate genes' gaped expression in NSCLC versus normal lung samples, and the results showed the gain of expression of all four genes in cancer comparing to normal samples (Figure 4B, 4D, 4F, 4H).

Further, multivariate cox regression analysis showed that patients age, p-stage, M status and NDC80 expression work as independent prognostic indicators in adenocarcinoma (Table 2), meanwhile, T stage, M status and MAD2L1 expression work as an independent indicators in squamous cell carcinoma (Table 3).

NDC80 and MAD2L1 association with NSCLC clinical features

To explore the clinical association between NDC80 and MAD2L1 expression with LUAD and LUSC clinical features, we used two methods. Firstly, the clinical information of 482 lung squamous cell carcinoma (Detailed in Table S1) and 223 adenocarcinoma cases (Table S2) were downloaded from TCGA data (same information being used for COX regression analysis), and the results showed that NDC80 expression statistical significantly associates with LUAD patients age, smoking, and stage in adenocarcinoma, the gene tends to express higher in younger (<60years), smoker and higher stage patients (Table 4). And MAD2L1 expression statistical significantly associates with LUSC lympho node and distant metastasis, the expression was higher in patients with lympho node metastasis but no distant metastasis (Table 5).

Secondly, an online analysis service Ualcan which is also based on TCGA data was also used for data exploration (Figure 5A-5N), the result also revealed that NDC80 expresses higher in smoker than non smokers and the expression increases as the smoking years lasting longer (Figure 5D), and NDC80 tends to be higher in cases with lympho node netastasis (Figure 5G). Interestingly, bigger sample number also yields the discovery that both NDC80 (Figure 5C) and MAD2LI (Figure 5J) express higher in male than female patients, hypothetically, the gender association might be related to the fact that most smokers were man rather than woman.

NDC80 and MAD2L1 centered signaling pathways

The expression profile of NDC80 and MAD2L1 was analyzed in various tumors using GEPIA and we discovered that both NDC80 and MAD2L1 were broad-spectrum up-regulated in multiple human tumors including lung adenocarcinoma and lung squamous cell carcinoma (Figure 6A, 6F).

To understand the potential functions of NDC80 and MAD2L1, we performed GO and KEGG to analyze the biological processes the genes mainly participate in and the signaling pathways they involve. The result revealed an really interesting fact that even in different sub types of lung cancer (LUAD and LUSC), NDC80 and MAD2L1 shared biological functions. Both

NDC80 (Table 6) and MAD2L1 (Table 7) were primarily focused on mitotic cell cycle regulation related processes, for instance cell division, chromosome segregation and spindle assembly regulating signaling.

Moreover, NDC80 and MAD2L1 centered PPI network showed a similar result that the genes NDC80 (Figure 6B) and MAD2L1 (Figure 6G) related were both cell cycle regulation involved including BUB1B and AURKA. GEPIA analysis confirmed the correlation between NDC80 and MAD2L1, BUB1B, AURKA in both LUAD (Figure 6C-6E) and LUSC (Figure 6H-6J).

Considering that great proportion of current chemotherapy drugs are developed based on their association with cell mitosis cycle, the correlation between NDC80, MAD2L1 and cell division process indicate the potential value these genes working as two other chemotherapy drug targets. However, more experiments and clinical trials will be needed to validate the hypothesis.

Discussion

Lung cancer has been the top killer among various malignant tumors worldwide, with the morbidity only second to prostatic cancer in male and breast cancer in female. Within the lung cancer, 80%~85% is NSCLC. Even with the rising of molecular targeted therapies, including EGFR, BRAF, C-MET, ALK, ROS1, RET and so on, the outcome of the disease is still not promising. The study is conducted to explore new potential biomarkers and gene targets by bioinformatic analyzing.

From the online open-access GEO databases, three cDNA expression profiles GSE44077, GSE18842 and GSE33532 containing a total of 181 NSCLC cancer and 131 normal lung samples were picked, and the GDEs between cancer versus normal tissues were then analyzed, and we discovered that 664 genes were differently expressed in three cDNA profiles, including 232 up-regulated and 432 down-regulated genes.

Then, we performed GO and KEGG analysis to annotate the 664 GDEs, and the results showed that the cell component that the 432 down-regulated genes mainly enriched in were plasma membrane, the biological processes the genes focused on were signal transduction and cell communication. The molecular functions that genes enriched in were receptor activity and cell adhesion molecular activity. Meanwhile, the biological pathways that down-regulated GDEs mostly enriched in were hemostasis and cell surface interaction at vascular walls.

To provoke our interests, three out of the four aspects the 232 up-regulated GDEs, including their cell growth and maintenance, spindle assembly and chromosome segregation enriched biological process, centrosome, microtubule and kinetochore centralized cell components and cell cycle/mitotic and DNA replication focused biological pathways point to the orientation of cell cycle mitotic process.

On top of it, the function modules analysis of GDEs revealed that most of the top module genes were also cell cycle regulation related. Overall survival analysis showed 17/31 of the top module genes statistical significantly correlate with NSCLC OS including four spindle assemble checkpoints NDC80, BUB1B, MAD2L1 and AURKA. Multivariate COX regression analysis supported NDC80 and MAD2L1 working as independent prognostic indicators in LUAD and LUSC respectively. Clinical features association analysis showed that NDC80 tends to expresses higher in younger (<60years) LUAD patients who smoke. And MAD2L1 usually expresses higher in LUSC patients with lympho node metastasis. Moreover, NDC80 and MAD2L1 centered biological processes and signaling pathways also highly support their involvement in the cell cycle regulation.

In fact, cell cycle regulators have been strongly implicated in the progression of various tumors^{26,27}, and disruption of cell cycle pathways including spindle assembly has been one of the main focus of current development of chemotherapy drugs²⁸⁻³⁰, for instance taxol and colchicine, which disrupts the microtubule polymerization dynamics, leading to inordinate spindle function and eventually cell death³¹⁻³⁴.

The over expression of multiple spindle checkpoints is revealing another potential microtubule-targeted strategy, the direct attack to spindle assemble checkpoint function, to arrest the cell cycle process in the prometaphase, thus leading to mitotic catastrophe and eventually cancer cell death.

NDC80, which is short for nuclear division cycle 80, is one of the proteins of outer kinetochore. It forms a heterotetramer complex with proteins SPC24, SPC25 and NUF2, and the complex has been known to involve in spindle assembly checkpoint signaling, detecting the unaligned chromosomes to assure the correct segregation of chromosomes. Aberrant expression of NDC80 has been reported in several other tumors³⁸⁻⁴², for instance osteosarcoma, hepatocellular carcinoma, colorectal cancer and breast cancer, indicating its potential as a newly bio target.

MAD2L1, short for mitosis arrest-deficient 2 like 1 protein, is also functioning as a spindle assembly checkpoint that assures the properly alignment of chromosomes at the metaphase plate during cell division. Despite the barely known signaling pathways it participated in, MAD2L1 is shown to interact with CDC20 and BUB1B^{43,44}, and correlate with aberrant development of salivary duct carcinoma⁴⁵.

BUB1, which is encoded by BUB1B, has been known as a checkpoint for proper chromosome segregation, the abnormal expression of BUB1 has been reported to associate with poor survival and metastasis in various tumors including colorectal cancer, gastric cancer, bladder cancer, hepatocellular carcinoma and so on³⁵⁻³⁸. In the study, using bioinformatic analysis, we confirmed the correlation between over expression of BUB1B and poor survival of NSCLC patients.

Aurora kinase A (AURKA) belongs on a family of [serine/threonine kinases](#) containing other two family members aurora kinase B and kinase C. The family members are known to have highly conserved genetic domains and shown to play vital roles in mitosis. As a [serine/threonine kinases](#), AURKA activity peaks during the G2/M [phase](#) transition phase in the cell cycle, and associated with the regulation of spindle stability. Aurora A dysregulation has been associated with high occurrence of various cancers, for example breast, prostate, bladder, colorectal, gastric, ovarian, esophagus and pancreatic cancers. High expression of AURKA commonly correlates with advanced development and poor prognosis of cancers⁴⁶⁻⁴⁸. [Osimertinib](#) and [rociletinib](#), two anti-cancer drugs for [lung cancer](#), work by shutting off mutant [EGFR](#)⁴⁹, which initially kills cancerous tumors, but the tumors rewire and activate Aurora kinase A, becoming cancerous growths again^{50,51}. A recent study shows that to target both EGFR and Aurora shall prevents return of drug resistant tumors⁵²⁻⁵⁴.

Further clinical validation of the tumor promoter and worse prognosis predictor function of NDC80 and MAD2L1 in local LUAD and LUSC patients as well as the genes' relation with BUB1B and AURKA is on our way. More experimental investigations are needed to understand the detailed molecular signaling mechanism behind the cell cycle related genes regulation on NSCLC development.

Conclusion

In conclusion, 664 GDEs between NSCLC and normal lung tissues were explored using bioinformatic analysis, and the cellular components, molecular functions, biological processes and the signaling they mainly enriched in were also revealed. Two spindle assembly checkpoints NDC80 and MAD2L1 were showed to correlate with LUAD and LUSC OS respectively. These bioinformation shall provide clues for the further unearthing of new biomarkers and potential bio-targets in NSCLC.

List Of Abbreviations

NSCLC Non-Small Cell Lung Cancer

LUAD Lung adenocarcinoma

LUSC Lung squamous cell carcinoma

GEO Gene Expression Omnibus
GDEs Genes with different expression level
GO Gene ontology
OS overall survival rate
KEGG Kyoto Encyclopedia of Gene and Genome
PPI protein-protein interaction network
MCODE Molecular Complex Detection
STRING Search Tool for Retrieval of interacting Genes
EMT Epithelial to Mesenchymal transition

Declarations

Ethics approval and consent to participate

Not applicable.

Consent for publication

Not applicable.

Availability of data and materials

In the study, different web-based datasets were used for data analysis. The web links to all the original data sources were listed as below: Three cDNA expression files GSE44077 (based on GPL6244[*HuGene-1_0-st*] Affymetrix Human Gene 1.0 ST Array. Web link: <https://www.ncbi.nlm.nih.gov/geo/query/acc.cgi?acc=GSE44077>), GSE18842 (based on GPL570[*HG-U133_Plus_2*] Affymetrix Human Genome U133 Plus 2.0 Array. Web link: <https://www.ncbi.nlm.nih.gov/geo/query/acc.cgi?acc=GSE18842>) and GSE33532 (based on GPL570[*HG-U133_Plus_2*] Affymetrix Human Genome U133 Plus 2.0 Array. Web link: <https://www.ncbi.nlm.nih.gov/geo/query/acc.cgi?acc=GSE33532>) were downloaded from Gene Expression Omnibus (GEO). And during the survival analysis of genes, 223 lung adenocarcinoma and 482 lung squamous cell carcinoma data were obtained from The Cancer Genome Atlas Program (TCGA) (Detailed in Supplementary Table 1 and Supplementary Table 2), meanwhile another analysis was conducted based on UALCAN (an interactive web resource for analyzing cancer transcriptome data. Web link: <http://ualcan.path.uab.edu/analysis.html>) provided lung adenocarcinoma and squamous cell carcinoma data. All data generated from the analysis process of this study are available from the corresponding author on reasonable request.

Competing interests

All of the authors approved the publication of the paper and declared no conflicts of interests. And as one of the corresponding author of the manuscript, Dr. Chen Wang works also as an associate editor of BMC Medical Genomics, we honestly declare that the whole process of manuscript reviewing was open, fair and impartial, absolutely no bias existed.

Funding

All the genetic analyzing and data processing work was supported by the grant of Health Commission of ShanXi Province in China to Chen Wang (NO.2018050).

Authors' contributions

RW, ZW designed the study and drafted the manuscript, contributed equally to the whole study. YZ, BW and NS worked on the data collection and acquisition, and they also led the data analysis in the whole study. LE, XL and LS performed the data interpretation and assisted the study design, YS, WY and XZ assisted manuscript revising and figures organizing. As the corresponding author, WM and CW were responsible for critical revision of the manuscript and have full access to all data generated from the project. All listed authors read and approved the final version of manuscript for publication.

Acknowledgements

We sincerely appreciate the researchers for providing their GEO and TCGA databases information online, we are truly honored to acknowledge their contributions.

Reference

1. Torre LA, Bray F, Siegel RL, Ferlay J, Lortet-Tieulent J, Jemal A. Global cancer statistics, 2012. *CA Cancer J Clin.* 2015;65(2):87-108.
2. Siegel RL, Miller KD, Jemal A. Cancer Statistics, 2017. *CA Cancer J Clin.* 2017;67(1):7-30.
3. Wakelee H, Kelly K, Edelman MJ. 50 Years of progress in the systemic therapy of non-small cell lung cancer. *Am Soc Clin Oncol Educ Book.* 2014:177-189.
4. Spiro SG, Silvestri GA. One hundred years of lung cancer. *Am J Respir Crit Care Med.* 2005;172(5):523-529.
5. Stella GM, Luisetti M, Pozzi E, Comoglio PM. Oncogenes in non-small-cell lung cancer: emerging connections and novel therapeutic dynamics. *Lancet Respir Med.* 2013;1(3):251-261.
6. Paez JG, Janne PA, Lee JC, et al. EGFR mutations in lung cancer: correlation with clinical response to gefitinib therapy. *Science.* 2004;304(5676):1497-1500.
7. Mitsudomi T, Yatabe Y. Mutations of the epidermal growth factor receptor gene and related genes as determinants of epidermal growth factor receptor tyrosine kinase inhibitors sensitivity in lung cancer. *Cancer Sci.* 2007;98(12):1817-1824.
8. Tsao MS, Sakurada A, Cutz JC, et al. Erlotinib in lung cancer - molecular and clinical predictors of outcome. *N Engl J Med.* 2005;353(2):133-144.
9. Shaw AT, Felip E, Bauer TM, et al. Lorlatinib in non-small-cell lung cancer with ALK or ROS1 rearrangement: an international, multicentre, open-label, single-arm first-in-man phase 1 trial. *Lancet Oncol.* 2017;18(12):1590-1599.
10. Soda M, Choi YL, Enomoto M, et al. Identification of the transforming EML4-ALK fusion gene in non-small-cell lung cancer. *Nature.* 2007;448(7153):561-566.
11. Croegaert K, Kolesar JM. Role of anaplastic lymphoma kinase inhibition in the treatment of non-small-cell lung cancer. *Am J Health Syst Pharm.* 2015;72(17):1456-1462.
12. Gerber DE, Minna JD. ALK inhibition for non-small cell lung cancer: from discovery to therapy in record time. *Cancer Cell.* 2010;18(6):548-551.
13. Botling J, Edlund K, Lohr M, et al. Biomarker discovery in non-small cell lung cancer: integrating gene expression profiling, meta-analysis, and tissue microarray validation. *Clin Cancer Res.* 2013;19(1):194-204.
14. Aibar S, Abaigar M, Campos-Laborie FJ, Sanchez-Santos JM, Hernandez-Rivas JM, De Las Rivas J. Identification of expression patterns in the progression of disease stages by integration of transcriptomic data. *BMC Bioinformatics.* 2016;17(Suppl 15):432.
15. Kadara H, Fujimoto J, Yoo SY, et al. Transcriptomic architecture of the adjacent airway field cancerization in non-small cell lung cancer. *J Natl Cancer Inst.* 2014;106(3):dju004.

16. Sanchez-Palencia A, Gomez-Morales M, Gomez-Capilla JA, et al. Gene expression profiling reveals novel biomarkers in nonsmall cell lung cancer. *Int J Cancer*. 2011;129(2):355-364.
17. Meister M, Belousov A, EC X, et al. Intra-tumor Heterogeneity of Gene Expression Profiles in Early Stage Non-Small Cell Lung Cancer. *Journal of Bioinformatics Research Studies*. 2014.
18. Gene Expression Omnibus DataSets. <https://www.ncbi.nlm.nih.gov/gds/?term=>.
19. GEO2R. <https://www.ncbi.nlm.nih.gov/geo/geo2r/>. Accessed 4 May 2018.
20. FunRich software. <http://funrich.org/download>. Accessed 6 April 2018.
21. Search Tool for the Retrieval of interacting Genes. <https://string-db.org/>. Accessed 5 May 2018.
22. Cytoscape3.6.0 software. <http://www.softpedia.com/get/Science-CAD/Cytoscape.shtml>. Accessed 28 May 2018.
23. Kaplan Meier Plotter Survival analysis. <http://kmplot.com/analysis/>. Accessed 15 June 2018.
24. National cancer institute <https://www.cancer.gov/about-nci/organization/ccg/research/structural-genomics/tcga>. Accessed 09 Sep 2019.
25. Gene Expression Profiling Interactive Analysis. <http://gepia.cancer-pku.cn/>. Accessed 8 May 2018.
26. P S, J B, A L. Online survival analysis software to assess the prognostic value of biomarkers using transcriptomic data in non-small-cell lung cancer. *PloS one*. 2013;8(12):e82241.
27. Human Protein Atlas. <https://www.proteinatlas.org/>. Accessed 10 Jun 2018.
28. Bendris N, Lemmers B, Blanchard JM. Cell cycle, cytoskeleton dynamics and beyond: the many functions of cyclins and CDK inhibitors. *Cell Cycle*. 2015;14(12):1786-1798.
29. Vermeulen K, Van Bockstaele DR, Berneman ZN. The cell cycle: a review of regulation, deregulation and therapeutic targets in cancer. *Cell Prolif*. 2003;36(3):131-149.
30. Ingham M, Schwartz GK. Cell-Cycle Therapeutics Come of Age. *J Clin Oncol*. 2017;35(25):2949-2959.
31. Kumar A, Sharma PR, Mondhe DM. Potential anticancer role of colchicine-based derivatives: an overview. *Anticancer Drugs*. 2017;28(3):250-262.
32. Marzo-Mas A, Barbier P, Breuzard G, et al. Interactions of long-chain homologues of colchicine with tubulin. *Eur J Med Chem*. 2017;126:526-535.
33. Weaver BA. How Taxol/paclitaxel kills cancer cells. *Mol Biol Cell*. 2014;25(18):2677-2681.
34. KA A, D Y, GB R, et al. Cytotoxicity of paclitaxel in breast cancer is due to chromosome missegregation on multipolar spindles. *Science translational medicine*. 2014;6(229):229ra243.
35. de Voer RM, Geurts van Kessel A, Weren RD, et al. Germline mutations in the spindle assembly checkpoint genes BUB1 and BUB3 are risk factors for colorectal cancer. *Gastroenterology*. 2013;145(3):544-547.
36. Tong H, Wang J, Chen H, Wang Z, Fan H, Ni Z. Transcriptomic analysis of gene expression profiles of stomach carcinoma reveal abnormal expression of mitotic components. *Life Sci*. 2017;170:41-49.
37. Martel-Frchet V, Keramidas M, Nurisso A, et al. IPP51, a chalcone acting as a microtubule inhibitor with in vivo antitumor activity against bladder carcinoma. *Oncotarget*. 2015;6(16):14669-14686.
38. Xu B, Xu T, Liu H, Min Q, Wang S, Song Q. MiR-490-5p Suppresses Cell Proliferation and Invasion by Targeting BUB1 in Hepatocellular Carcinoma Cells. *Pharmacology*. 2017;100(5-6):269-282.
39. Xu B, Wu DP, Xie RT, Liu LG, Yan XB. Elevated NDC80 expression is associated with poor prognosis in osteosarcoma patients. *Eur Rev Med Pharmacol Sci*. 2017;21(9):2045-2053.
40. Ju LL, Chen L, Li JH, et al. Effect of NDC80 in human hepatocellular carcinoma. *World J Gastroenterol*. 2017;23(20):3675-3683.
41. Yan X, Huang L, Liu L, Qin H, Song Z. Nuclear division cycle 80 promotes malignant progression and predicts clinical outcome in colorectal cancer. *Cancer Med*. 2018;7(2):420-432.

42. Bieche I, Vacher S, Lallemand F, et al. Expression analysis of mitotic spindle checkpoint genes in breast carcinoma: role of NDC80/HEC1 in early breast tumorigenicity, and a two-gene signature for aneuploidy. *Mol Cancer*. 2011;10:23.
43. Vleugel M, Hoek TA, Tromer E, et al. Dissecting the roles of human BUB1 in the spindle assembly checkpoint. *J Cell Sci*. 2015;128(16):2975-2982.
44. Abal M, Obrador-Hevia A, Janssen KP, et al. APC inactivation associates with abnormal mitosis completion and concomitant BUB1B/MAD2L1 up-regulation. *Gastroenterology*. 2007;132(7):2448-2458.
45. Ko YH, Roh JH, Son YI, et al. Expression of mitotic checkpoint proteins BUB1B and MAD2L1 in salivary duct carcinomas. *J Oral Pathol Med*. 2010;39(4):349-355.
46. Hasanov E, Chen G, Chowdhury P, et al. Ubiquitination and regulation of AURKA identifies a hypoxia-independent E3 ligase activity of VHL. *Oncogene*. 2017;36(24):3450-3463.
47. Chen C, Song G, Xiang J, Zhang H, Zhao S, Zhan Y. AURKA promotes cancer metastasis by regulating epithelial-mesenchymal transition and cancer stem cell properties in hepatocellular carcinoma. *Biochem Biophys Res Commun*. 2017;486(2):514-520.
48. Puig-Butille JA, Vinyals A, Ferreres JR, et al. AURKA Overexpression Is Driven by FOXM1 and MAPK/ERK Activation in Melanoma Cells Harboring BRAF or NRAS Mutations: Impact on Melanoma Prognosis and Therapy. *J Invest Dermatol*. 2017;137(6):1297-1310.
49. Song Z, Ge Y, Wang C, et al. Challenges and Perspectives on the Development of Small-Molecule EGFR Inhibitors against T790M-Mediated Resistance in Non-Small-Cell Lung Cancer. *J Med Chem*. 2016;59(14):6580-6594.
50. Chong CR, Janne PA. The quest to overcome resistance to EGFR-targeted therapies in cancer. *Nat Med*. 2013;19(11):1389-1400.
51. Chen J, Lu H, Zhou W, et al. AURKA upregulation plays a role in fibroblast-reduced gefitinib sensitivity in the NSCLC cell line HCC827. *Oncol Rep*. 2015;33(4):1860-1866.
52. Astsaturov I, Ratushny V, Sukhanova A, et al. Synthetic lethal screen of an EGFR-centered network to improve targeted therapies. *Sci Signal*. 2010;3(140):ra67.
53. Kurup S, McAllister B, Liskova P, et al. Design, synthesis and biological activity of N(4)-phenylsubstituted-7H-pyrrolo[2,3-d]pyrimidin-4-amines as dual inhibitors of aurora kinase A and epidermal growth factor receptor kinase. *J Enzyme Inhib Med Chem*. 2018;33(1):74-84.
54. Shah KN, Bhatt R, Rotow J, et al. Aurora kinase A drives the evolution of resistance to third-generation EGFR inhibitors in lung cancer. *Nat Med*. 2018.

Tables

Table 1. Signaling pathways that Cluster 1 genes mainly enriched in.

*Only pathways containing over 10 GDEs were listed.

Table 2 Multivariate cox regression analysis on LUAD overall survival

Variables	Lung adenocarcinoma		
	Hazard ratio	95% CI	P value
Age <60 years vs ≥60 years	1.034	1.006~1.064	0.018
Stage I vs II vs III vs IV	1.554	1.213~1.99	0.001
M M ₀ vs M ₁	2.321	1.172~4.069	0.032
NDC80 expression <median vs >median	2.480	1.375~4.472	0.003

pathways	count	P value	Related GDEs in the network
Cell Cycle, Mitotic	31	2.76403E-29	CENPE; KNTC1; KIF18A; TOP2A; MAD2L1; CCNB2; CKS1B; MCM4; CCNB1; PTTG1; NUF2; CDK1; AURKA; PLK1; TYMS; CCNA2; CDC20; NDC80; BUB1; CDC6; GINS2; CDC45; PLK4; CDCA8; KIF20A; RRM2; KIF2C; RFC4; KIF23; CENPF; NEK2;
DNA Replication	22	1.71367E-18	CENPE; KNTC1; KIF18A; MAD2L1; MCM4; NUF2; CDK1; PLK1; CDC20; NDC80; BUB1; CDC6; GINS2; CDC45; PLK4; CDCA8; KIF20A; KIF2C; RFC4; KIF23; CENPF; NEK2;
Mitotic M-M/G1 phases	20	1.48601E-16	CENPE; KNTC1; KIF18A; MAD2L1; MCM4; NUF2; CDK1; PLK1; CDC20; NDC80; BUB1; CDC6; CDC45; PLK4; CDCA8; KIF20A; KIF2C; KIF23; CENPF; NEK2;
M Phase	17	5.76137E-16	CENPE; KNTC1; KIF18A; MAD2L1; NUF2; CDK1; PLK1; CDC20; NDC80; BUB1; PLK4; CDCA8; KIF20A; KIF2C; KIF23; CENPF; NEK2;
Polo-like kinase signaling events in the cell cycle	14	2.77681E-14	CENPE; CCNB1; CDK1; AURKA; TPX2; ECT2; PLK1; PRC1; CDC20; NDC80; BUB1; PLK4; DLGAP5; KIF20A;
PLK1 signaling events	13	3.83583E-13	CENPE; CCNB1; CDK1; AURKA; TPX2; ECT2; PLK1; PRC1; CDC20; NDC80; BUB1; DLGAP5; KIF20A;
Mitotic Prometaphase	12	5.11023E-12	CENPE; KNTC1; KIF18A; MAD2L1; NUF2; PLK1; CDC20; NDC80; BUB1; CDCA8; KIF2C; CENPF;
Cell Cycle Checkpoints	11	1.32039E-08	MAD2L1; CCNB2; MCM4; NDC80; CCNB1; CDK1; CDC20; CDC6; CDC45; RFC4; CHEK1;
Signaling by Aurora kinases	11	1.04137E-10	NCAPH; NCAPG; AURKA; TPX2; NDC80; BUB1; CDCA8; DLGAP5; KIF20A; KIF2C; KIF23;

Table 3 Multivariate cox regression analysis on LUSC overall survival

Variables	Lung squamous cell carcinoma		
	Hazard ratio	95% CI	P value
T T1 vs T2 vs T3 vs T4	1.305	1.085~1.569	0.005
M M ₀ vs M ₁	1.701	1.172~2.469	0.005
MAD2L1 expression <median vs >median	0.753	0.567~0.999	0.045

Table 4 The association between NDC80 and LUAD clinical pathological features

parameters	NDC80		P value
	-	+	
Gender			P=0.209
male	45 (45.9%)	53 (54.1%)	
female	68 (54.4%)	57 (45.6%)	
Age			P=0.027
< 60 years old	24 (39.3%)	37 (60.7%)	
≥ 60 years old	82 (56.2%)	64 (43.8%)	
Smoke			P=0.002
no	23 (65.7%)	12 (34.3%)	
Current smoker	15 (32.6%)	31 (67.4%)	
Smoker <15 years	31 (44.9%)	38 (55.1%)	
Smoker ≥15 years	39 (59.1%)	27 (40.9%)	
Stage			P=0.032
I	66 (57.4%)	49 (42.6%)	
II	23 (48.9%)	24 (51.1%)	
III	15 (31.9%)	32 (68.2%)	
IV	5 (55.6%)	4 (44.4%)	
T			P=0.199
I	37 (61.7%)	23 (38.3%)	
II	63 (47.7%)	68 (52.3%)	
III	7 (41.2%)	10 (58.8%)	
IV	6 (40.0%)	9 (60.0%)	
N			P=0.053
-	69 (56.6%)	53 (43.4%)	
+	44 (43.6%)	57 (56.4%)	
M			P=0.497
-	81 (50.9%)	78 (49.1%)	
+	27 (45.8%)	31 (54.2%)	

Table 5 The association between MAD2L1 and LUSC clinical pathological features

parameters	MAD2L1		P value
	-	+	
Gender			P=0.097
male	170 (47.8%)	186 (52.2%)	
female	71 (56.3%)	55 (43.7%)	
Age			P=0.100
< 60 years old	44 (42.7%)	59 (57.3%)	
≥ 60 years old	192 (51.9%)	178 (48.1%)	
Smoke			P=0.973
no	131 (50.6%)	128 (49.4%)	
Smoker <15 years	28 (50.0%)	28 (50.0%)	
Smoker ≥15 years	82 (49.4%)	84 (50.6%)	
Stage			P=0.062
I	132 (56.2%)	103 (43.8%)	
II	70 (44.6%)	87 (55.4%)	
III	35 (42.7%)	47 (57.3%)	
IV	4 (57.1%)	3 (42.9%)	
T			P=0.314
I	60 (56.1%)	47 (43.9%)	
II	131 (46.5%)	151 (53.5%)	
III	38 (54.3%)	32 (45.7%)	
IV	12 (52.2%)	11 (47.8%)	
N			P=0.001
-	171 (55.9%)	135 (44.1%)	
+	70 (39.8%)	106 (60.2%)	
M			P=0.036
-	188 (48.0%)	204 (52.0%)	
+	52 (60.5%)	34 (39.5%)	

Table 6 Go analysis revealing biological processes centered on NDC80

Description	Gene counts	Background gene counts	FDR	Matching proteins in the network
Cell division	11	483	7.33E-16	AURKB,BUB1,BUB1B,CASC5,NUF2,CENPE,MAD2L1,NDC80,SPC24,SPC25,ZWINT
Chromosome segregation	10	253	7.33E-16	AURKB,BUB1,BUB1B,CASC5,CENPE,MAD2L1,NDC80,NUF2,SPC25,ZWINT
Sister chromatid segregation	7	123	1.31E-11	AURKB,BUB1,BUB1B,CENPE,MAD2L1,NDC80,ZWINT
Spindle attachment to kinetochore	4	20	1.32E-08	AURKB,CASC5,CENPE,NDC80
Spindle checkpoint	4	23	2.07E-08	AURKB,BUB1,BUB1B,MAD2L1

Table 7 Go analysis revealing biological processes centered on MAD2L1

Description	Gene counts	Background gene counts	FDR	Matching proteins in the network
Cell division	10	483	1.09E-15	ANAPC1,ANAPC4,BUB1,BUB1B,BUB3,CDC16,CDC20,MAD1L1,MAD2L1,NEK2
Nuclear division regulation	9	184	9.05E-15	ANAPC4,BUB1,NEK2,BUB1B,BUB3,CDC16,CDC20,MAD1L1,MAD2L1
Chromosome organization	8	999	6.17E-08	BUB1,BUB1B,BUB3,CCNA2,CDC20,MAD1L1,MAD2L1,NEK2
anaphase-promoting complex-dependent catabolic process	7	35	9.05E-15	ANAPC1,ANAPC4,BUB1B,BUB3,CDC16,CDC20,MAD2L1
Mitotic spindle assembly checkpoint	5	21	4.46E-11	BUB1,BUB1B,BUB3,MAD1L1,MAD2L1

Supplementary Tables

Supplementary Table 1 The TCGA patients barcode for 482 LUSC samples

TCGA-18-3406	TCGA-18-3419	TCGA-21-5784	TCGA-22-5479	TCGA-33-4587	TCGA-37-5819
TCGA-18-3407	TCGA-18-3421	TCGA-21-5786	TCGA-22-5480	TCGA-33-4589	TCGA-37-A5EL
TCGA-18-3408	TCGA-18-4083	TCGA-21-5787	TCGA-22-5481	TCGA-33-6737	TCGA-37-A5EM
TCGA-18-3409	TCGA-18-4086	TCGA-21-A5DI	TCGA-22-5482	TCGA-33-6738	TCGA-37-A5EN
TCGA-18-3410	TCGA-18-4721	TCGA-22-0940	TCGA-22-5483	TCGA-33-A4WN	TCGA-39-5011
TCGA-18-3411	TCGA-18-5592	TCGA-22-0944	TCGA-22-5485	TCGA-33-A5GW	TCGA-39-5016
TCGA-18-3412	TCGA-18-5595	TCGA-22-1000	TCGA-22-5489	TCGA-33-AAS8	TCGA-39-5019
TCGA-18-3414	TCGA-21-1070	TCGA-22-1002	TCGA-22-5491	TCGA-33-AASB	TCGA-39-5021
TCGA-18-3415	TCGA-21-1071	TCGA-22-1005	TCGA-22-5492	TCGA-33-AASD	TCGA-39-5022
TCGA-18-3416	TCGA-21-1072	TCGA-22-1011	TCGA-22-A5C4	TCGA-33-AASI	TCGA-39-5024
TCGA-18-3417	TCGA-21-1075	TCGA-22-1012	TCGA-33-4532	TCGA-33-AASJ	TCGA-39-5027
TCGA-56-8622	TCGA-21-1076	TCGA-22-1016	TCGA-33-4533	TCGA-33-AASL	TCGA-39-5028
TCGA-56-8623	TCGA-21-1077	TCGA-22-1017	TCGA-33-4538	TCGA-34-2596	TCGA-39-5029
TCGA-56-8624	TCGA-21-1078	TCGA-22-4591	TCGA-33-4547	TCGA-34-2600	TCGA-39-5030
TCGA-56-8625	TCGA-21-1079	TCGA-22-4593	TCGA-33-4566	TCGA-34-2604	TCGA-39-5031
TCGA-56-8626	TCGA-21-1080	TCGA-22-4594	TCGA-33-4582	TCGA-34-2605	TCGA-39-5034
TCGA-56-8628	TCGA-21-1081	TCGA-22-4595	TCGA-33-4583	TCGA-34-2608	TCGA-39-5035
TCGA-56-8629	TCGA-21-1082	TCGA-22-4596	TCGA-33-4586	TCGA-34-2609	TCGA-39-5036
TCGA-56-A49D	TCGA-21-1083	TCGA-22-4599	TCGA-37-4133	TCGA-34-5231	TCGA-39-5037
TCGA-56-A4BW	TCGA-21-5782	TCGA-22-4601	TCGA-37-4135	TCGA-34-5232	TCGA-39-5039
TCGA-56-A4BX	TCGA-21-5783	TCGA-22-4604	TCGA-37-4141	TCGA-34-5234	TCGA-39-5040
TCGA-56-A4BY	TCGA-60-2695	TCGA-22-4605	TCGA-43-A474	TCGA-34-5236	TCGA-43-2576
TCGA-56-A4ZJ	TCGA-60-2696	TCGA-22-4607	TCGA-43-A475	TCGA-34-5239	TCGA-43-2578
TCGA-56-A4ZK	TCGA-60-2697	TCGA-22-4609	TCGA-43-A56U	TCGA-34-5240	TCGA-43-2581
TCGA-56-A5DR	TCGA-60-2698	TCGA-22-4613	TCGA-56-8309	TCGA-34-5241	TCGA-43-3394
TCGA-56-A5DS	TCGA-60-2703	TCGA-22-5471	TCGA-56-8503	TCGA-34-5927	TCGA-43-3920
TCGA-56-A62T	TCGA-60-2704	TCGA-22-5472	TCGA-56-8504	TCGA-34-5928	TCGA-43-5668
TCGA-58-8386	TCGA-60-2706	TCGA-22-5473	TCGA-63-5131	TCGA-34-5929	TCGA-43-5670
TCGA-58-8387	TCGA-60-2707	TCGA-22-5474	TCGA-63-6202	TCGA-34-7107	TCGA-43-6143
TCGA-58-8388	TCGA-60-2708	TCGA-22-5477	TCGA-63-7020	TCGA-34-8454	TCGA-43-6647
TCGA-58-8390	TCGA-60-2709	TCGA-22-5478	TCGA-63-7021	TCGA-34-8455	TCGA-43-6770
TCGA-58-8391	TCGA-60-2710	TCGA-60-2720	TCGA-63-7022	TCGA-34-8456	TCGA-43-6771
TCGA-58-8392	TCGA-60-2711	TCGA-60-2721	TCGA-63-7023	TCGA-34-A5IX	TCGA-43-6773
TCGA-58-8393	TCGA-60-2712	TCGA-60-2722	TCGA-63-A5M9	TCGA-37-3783	TCGA-43-7656
TCGA-58-A46J	TCGA-60-2713	TCGA-60-2723	TCGA-63-A5MB	TCGA-37-3789	TCGA-43-7657
TCGA-58-A46K	TCGA-60-2714	TCGA-60-2724	TCGA-63-A5MG	TCGA-37-3792	TCGA-43-7658
TCGA-58-A46L	TCGA-60-2715	TCGA-60-2725	TCGA-63-A5MH	TCGA-37-4129	TCGA-43-8115
TCGA-58-A46M	TCGA-60-2716	TCGA-60-2726	TCGA-63-A5MI	TCGA-37-4130	TCGA-43-8116
TCGA-58-A46N	TCGA-60-2719	TCGA-63-5128	TCGA-63-A5MJ	TCGA-37-4132	TCGA-43-8118
TCGA-66-2755	TCGA-63-A5ML	TCGA-77-6842	TCGA-77-A5GF	TCGA-85-A4PA	TCGA-43-A56V
TCGA-66-2756	TCGA-63-A5MM	TCGA-77-6843	TCGA-77-A5GH	TCGA-85-A4QQ	TCGA-46-3765
TCGA-66-2757	TCGA-63-A5MN	TCGA-77-6844	TCGA-79-5596	TCGA-85-A4QR	TCGA-46-3766
TCGA-66-2758	TCGA-63-A5MP	TCGA-77-6845	TCGA-85-6175	TCGA-85-A50M	TCGA-46-3767
TCGA-66-2759	TCGA-63-A5MR	TCGA-77-7138	TCGA-85-6560	TCGA-85-A50Z	TCGA-46-3768
TCGA-66-2763	TCGA-63-A5MS	TCGA-77-7139	TCGA-85-6561	TCGA-85-A510	TCGA-46-3769
TCGA-66-2765	TCGA-63-A5MT	TCGA-77-7140	TCGA-85-6798	TCGA-85-A511	TCGA-46-6025
TCGA-66-2766	TCGA-63-A5MU	TCGA-77-7141	TCGA-85-7696	TCGA-85-A512	TCGA-46-6026
TCGA-66-2767	TCGA-63-A5MV	TCGA-77-7142	TCGA-85-7697	TCGA-85-A513	TCGA-51-4079
TCGA-66-2768	TCGA-63-A5MW	TCGA-77-7335	TCGA-85-7698	TCGA-85-A53L	TCGA-51-4080
TCGA-66-2769	TCGA-63-A5MY	TCGA-77-7337	TCGA-85-7699	TCGA-85-A5B5	TCGA-51-4081
TCGA-66-2770	TCGA-66-2727	TCGA-77-7338	TCGA-85-7710	TCGA-90-6837	TCGA-51-6867
TCGA-66-2771	TCGA-66-2734	TCGA-77-7463	TCGA-85-7843	TCGA-90-7766	TCGA-52-7622
TCGA-66-2773	TCGA-66-2737	TCGA-77-7465	TCGA-85-7844	TCGA-90-7767	TCGA-52-7809
TCGA-66-2777	TCGA-66-2742	TCGA-77-8007	TCGA-85-7950	TCGA-90-7769	TCGA-52-7810
TCGA-66-2778	TCGA-66-2744	TCGA-77-8008	TCGA-85-8048	TCGA-90-7964	TCGA-52-7811
TCGA-66-2780	TCGA-66-2753	TCGA-77-8009	TCGA-85-8049	TCGA-90-A4ED	TCGA-52-7812
TCGA-66-2781	TCGA-66-2754	TCGA-77-8128	TCGA-85-8052	TCGA-90-A4EE	TCGA-56-1622
TCGA-66-2782	TCGA-98-8022	TCGA-77-8130	TCGA-85-8070	TCGA-90-A59Q	TCGA-56-5897
TCGA-66-2783	TCGA-98-8023	TCGA-77-8131	TCGA-85-8071	TCGA-92-7340	TCGA-56-5898
TCGA-66-2785	TCGA-98-A538	TCGA-77-8133	TCGA-85-8072	TCGA-92-7341	TCGA-56-6545
TCGA-66-2786	TCGA-98-A539	TCGA-77-8136	TCGA-85-8276	TCGA-92-8063	TCGA-56-6546
TCGA-66-2787	TCGA-98-A53A	TCGA-77-8138	TCGA-85-8277	TCGA-92-8064	TCGA-56-7221
TCGA-66-2788	TCGA-98-A53B	TCGA-77-8139	TCGA-85-8287	TCGA-92-8065	TCGA-56-7222
TCGA-66-2789	TCGA-98-A53C	TCGA-77-8140	TCGA-85-8288	TCGA-94-7033	TCGA-56-7223
TCGA-66-2790	TCGA-98-A53D	TCGA-77-8143	TCGA-85-8350	TCGA-94-7557	TCGA-56-7579
TCGA-66-2791	TCGA-98-A53H	TCGA-77-8144	TCGA-85-8351	TCGA-94-7943	TCGA-56-7580
TCGA-66-2792	TCGA-98-A53I	TCGA-77-8145	TCGA-85-8352	TCGA-94-8035	TCGA-56-7582
TCGA-66-2793	TCGA-98-A53J	TCGA-77-8146	TCGA-85-8353	TCGA-94-8490	TCGA-56-7730
TCGA-66-2794	TCGA-J1-A4AH	TCGA-77-8148	TCGA-85-8354	TCGA-94-8491	TCGA-56-7731
TCGA-66-2795	TCGA-L3-A4E7	TCGA-77-8150	TCGA-85-8355	TCGA-94-A4VJ	TCGA-56-7822
TCGA-66-2800	TCGA-L3-A524	TCGA-77-8153	TCGA-85-8479	TCGA-94-A5I4	TCGA-56-7823

TCGA-68-7755	TCGA-LA-A446	TCGA-77-8154	TCGA-85-8481	TCGA-94-A5I6	TCGA-56-8082
TCGA-68-7756	TCGA-LA-A7SW	TCGA-77-8156	TCGA-85-8580	TCGA-96-7544	TCGA-56-8083
TCGA-68-7757	TCGA-MF-A522	TCGA-77-A5FZ	TCGA-85-8582	TCGA-96-7545	TCGA-56-8201
TCGA-68-8250	TCGA-NK-A5CT	TCGA-77-A5G1	TCGA-85-8584	TCGA-96-8169	TCGA-56-8304
TCGA-68-8251	TCGA-NK-A5CT	TCGA-77-A5G3	TCGA-85-8664	TCGA-96-8170	TCGA-56-8305
TCGA-68-A59I	TCGA-NK-A5CX	TCGA-77-A5G6	TCGA-85-8666	TCGA-96-A4JK	TCGA-56-8307
TCGA-68-A59J	TCGA-NK-A5D1	TCGA-77-A5G7	TCGA-85-A4CL	TCGA-96-A4JL	
TCGA-6A-AB49	TCGA-NK-A5D1	TCGA-77-A5G8	TCGA-85-A4CN	TCGA-98-7454	
TCGA-70-6722	TCGA-NK-A7XE	TCGA-77-A5GA	TCGA-85-A4JB	TCGA-98-8020	
TCGA-70-6723	TCGA-98-8021	TCGA-77-A5GB	TCGA-85-A4JC	TCGA-56-8308	

Supplementary Table 2 The TCGA patients barcode for 223 LUAD patients samples

TCGA-75-5125	TCGA-44-5643	TCGA-05-4430	TCGA-55-1592	TCGA-55-7576	TCGA-55-8092
TCGA-62-A471	TCGA-44-3917	TCGA-05-4424	TCGA-50-5045	TCGA-44-A4SS	TCGA-97-7554
TCGA-86-8358	TCGA-05-4402	TCGA-55-7995	TCGA-95-7947	TCGA-L9-A7SV	TCGA-44-8120
TCGA-05-4434	TCGA-69-7979	TCGA-95-8494	TCGA-55-8299	TCGA-62-8399	TCGA-4B-A93V
TCGA-05-4395	TCGA-62-A460	TCGA-44-2666	TCGA-80-5608	TCGA-49-AAR3	TCGA-55-A48Y
TCGA-73-4668	TCGA-05-4427	TCGA-05-5425	TCGA-49-6743	TCGA-55-8208	TCGA-78-7535
TCGA-78-7536	TCGA-86-A4JF	TCGA-69-7974	TCGA-69-7760	TCGA-86-8673	TCGA-50-5932
TCGA-50-5072	TCGA-78-7154	TCGA-62-8394	TCGA-05-4244	TCGA-55-A48Z	TCGA-55-7727
TCGA-64-5774	TCGA-49-4507	TCGA-55-7903	TCGA-05-4245	TCGA-44-5644	TCGA-44-A47B
TCGA-50-6591	TCGA-62-8402	TCGA-05-4382	TCGA-MP-A4TK	TCGA-73-4662	TCGA-44-A47F
TCGA-05-4398	TCGA-64-1676	TCGA-86-7713	TCGA-69-7980	TCGA-75-6205	TCGA-50-5939
TCGA-05-4418	TCGA-44-2656	TCGA-L9-A743	TCGA-75-5126	TCGA-05-4403	TCGA-95-7948
TCGA-44-7662	TCGA-44-4112	TCGA-78-7150	TCGA-73-A9RS	TCGA-99-8032	TCGA-05-4425
TCGA-55-1594	TCGA-99-8033	TCGA-55-1596	TCGA-MP-A4T4	TCGA-55-A494	TCGA-44-2655
TCGA-55-1595	TCGA-05-4422	TCGA-50-6594	TCGA-44-6775	TCGA-67-3772	TCGA-44-A47G
TCGA-38-4628	TCGA-80-5611	TCGA-44-7672	TCGA-69-7978	TCGA-44-7671	TCGA-97-A4LX
TCGA-73-7499	TCGA-50-6592	TCGA-MP-A4TC	TCGA-78-7160	TCGA-93-A4JN	TCGA-38-4627
TCGA-53-A4EZ	TCGA-69-7973	TCGA-86-7954	TCGA-55-8204	TCGA-64-5778	TCGA-91-6835
TCGA-86-8074	TCGA-86-7711	TCGA-91-6831	TCGA-MP-A4SY	TCGA-35-5375	
TCGA-49-AAR9	TCGA-05-4432	TCGA-99-8025	TCGA-MP-A4T2	TCGA-86-8279	
TCGA-NJ-A4YP	TCGA-05-4390	TCGA-64-1677	TCGA-86-8075	TCGA-80-5607	
TCGA-55-8205	TCGA-50-6590	TCGA-86-8073	TCGA-86-8278	TCGA-55-7914	
TCGA-64-5775	TCGA-55-6975	TCGA-MP-A4TI	TCGA-86-8055	TCGA-78-7147	
TCGA-55-8085	TCGA-49-6767	TCGA-55-7911	TCGA-55-8301	TCGA-L9-A8F4	
TCGA-62-8398	TCGA-75-6207	TCGA-05-4389	TCGA-86-6851	TCGA-49-4488	
TCGA-73-4676	TCGA-97-8176	TCGA-L9-A5IP	TCGA-64-1679	TCGA-55-8091	
TCGA-55-5899	TCGA-78-8660	TCGA-95-A4VN	TCGA-05-5420	TCGA-97-7553	
TCGA-95-7944	TCGA-78-7145	TCGA-55-8094	TCGA-78-8640	TCGA-44-2668	
TCGA-55-7994	TCGA-95-7567	TCGA-44-3919	TCGA-53-7626	TCGA-55-6983	
TCGA-78-7220	TCGA-78-7143	TCGA-78-7166	TCGA-50-5049	TCGA-62-A46Y	
TCGA-50-5946	TCGA-MN-A4N5	TCGA-MP-A4T8	TCGA-67-6215	TCGA-62-A46R	
TCGA-75-6214	TCGA-55-A4DF	TCGA-J2-A4AD	TCGA-MP-A4T7	TCGA-71-8520	
TCGA-50-5066	TCGA-49-4514	TCGA-05-5429	TCGA-55-8614	TCGA-97-8179	
TCGA-97-8175	TCGA-50-5068	TCGA-50-5933	TCGA-95-7043	TCGA-97-8177	
TCGA-73-4659	TCGA-93-A4JQ	TCGA-69-7761	TCGA-44-8117	TCGA-49-4487	
TCGA-55-8620	TCGA-05-4426	TCGA-78-7148	TCGA-97-8171	TCGA-67-3771	
TCGA-MP-A4SV	TCGA-55-8203	TCGA-MN-A4N1	TCGA-55-8302	TCGA-78-7153	
TCGA-55-6987	TCGA-44-7660	TCGA-NJ-A55R	TCGA-93-A4JP	TCGA-44-2665	
TCGA-53-7624	TCGA-MP-A4TA	TCGA-55-8090	TCGA-55-8511	TCGA-86-8280	
TCGA-44-3918	TCGA-75-5122	TCGA-69-A59K	TCGA-75-6211	TCGA-50-7109	
TCGA-78-7159	TCGA-49-AAQV	TCGA-95-8039	TCGA-MP-A4TE	TCGA-L4-A4E5	

Figures

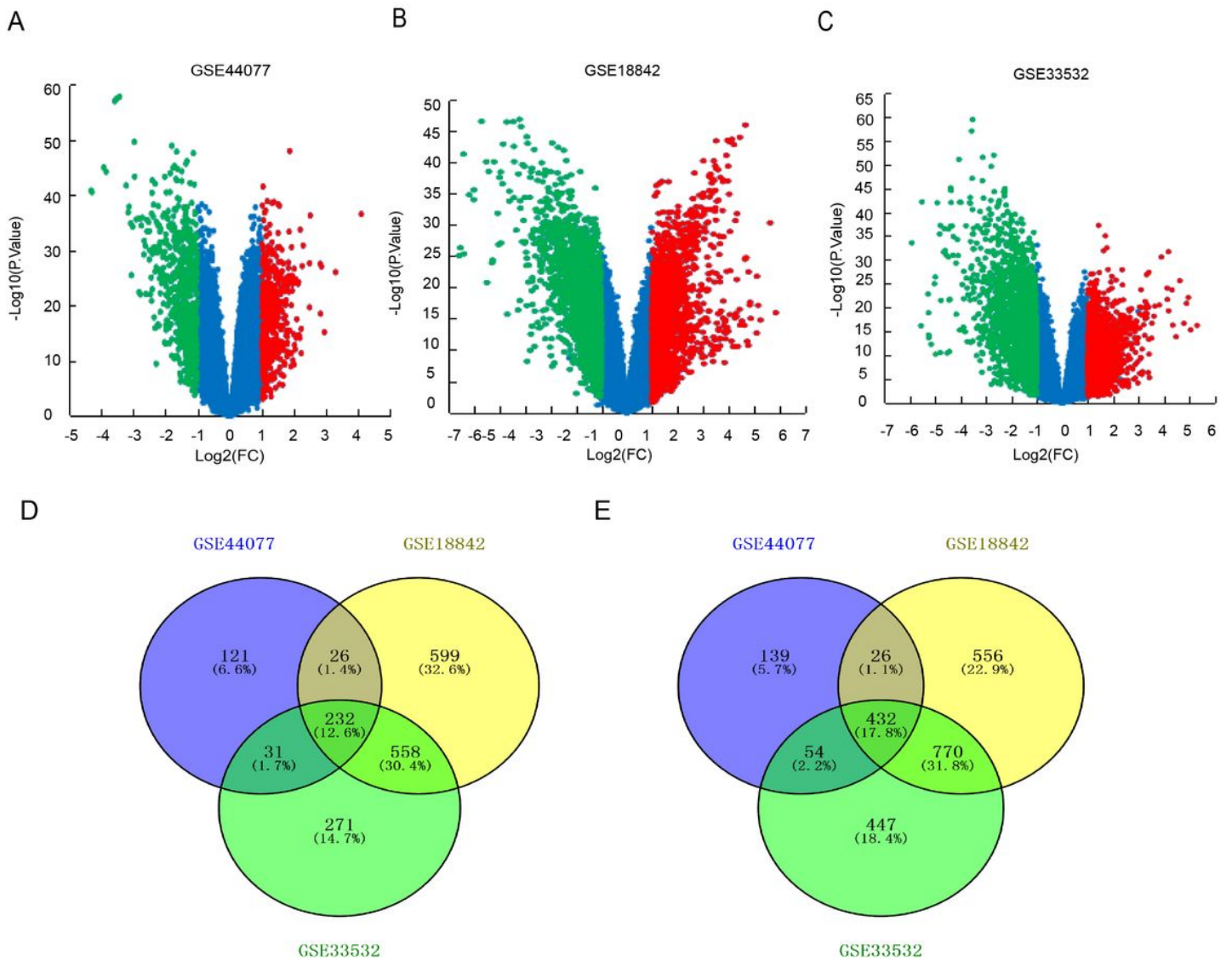


Figure 1

The GDEs analyzed by three GEO expression profiles. Up-regulated (red-colored) and down-regulated (green-colored) GDEs in NSCLC versus normal lung tissues analyzed based on GEO profiles (A) GSE44077, (B) GSE18842 and (C) GSE33532 respectively. (D) 232 up-regulated GDEs and (E) 432 down-regulated GDEs were shared in three cDNA expression profiles.

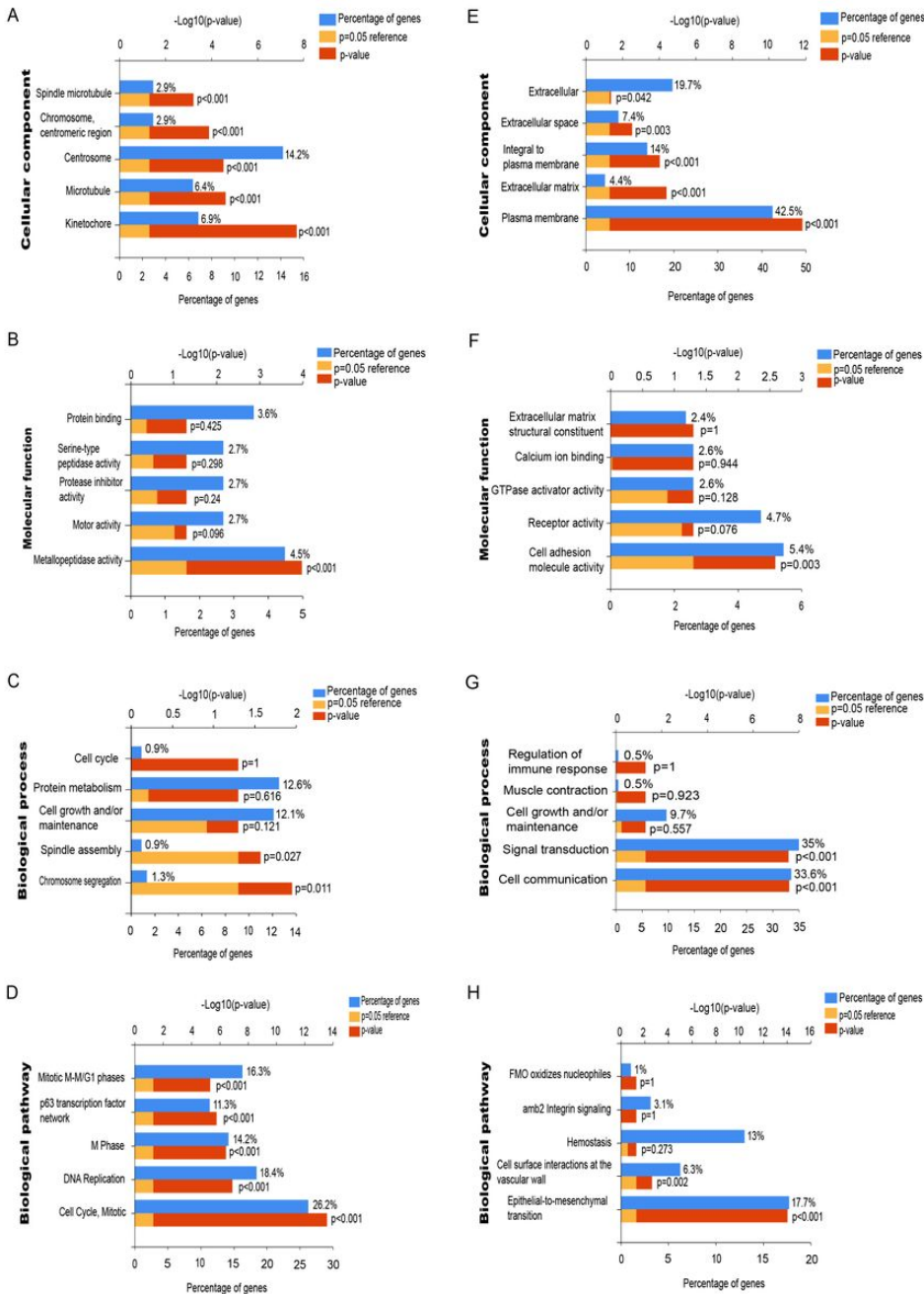


Figure 2

GDEs function analysis by GO and KEGG in NSCLC. (A) The cellular components, (B) molecular functions, (C) biological processes, and (D) biological pathways the up-regulated GDEs were enriched in. (A) The cellular components, (B) molecular functions, (C) biological processes, and (D) biological pathways the down-regulated GDEs were enriched in.

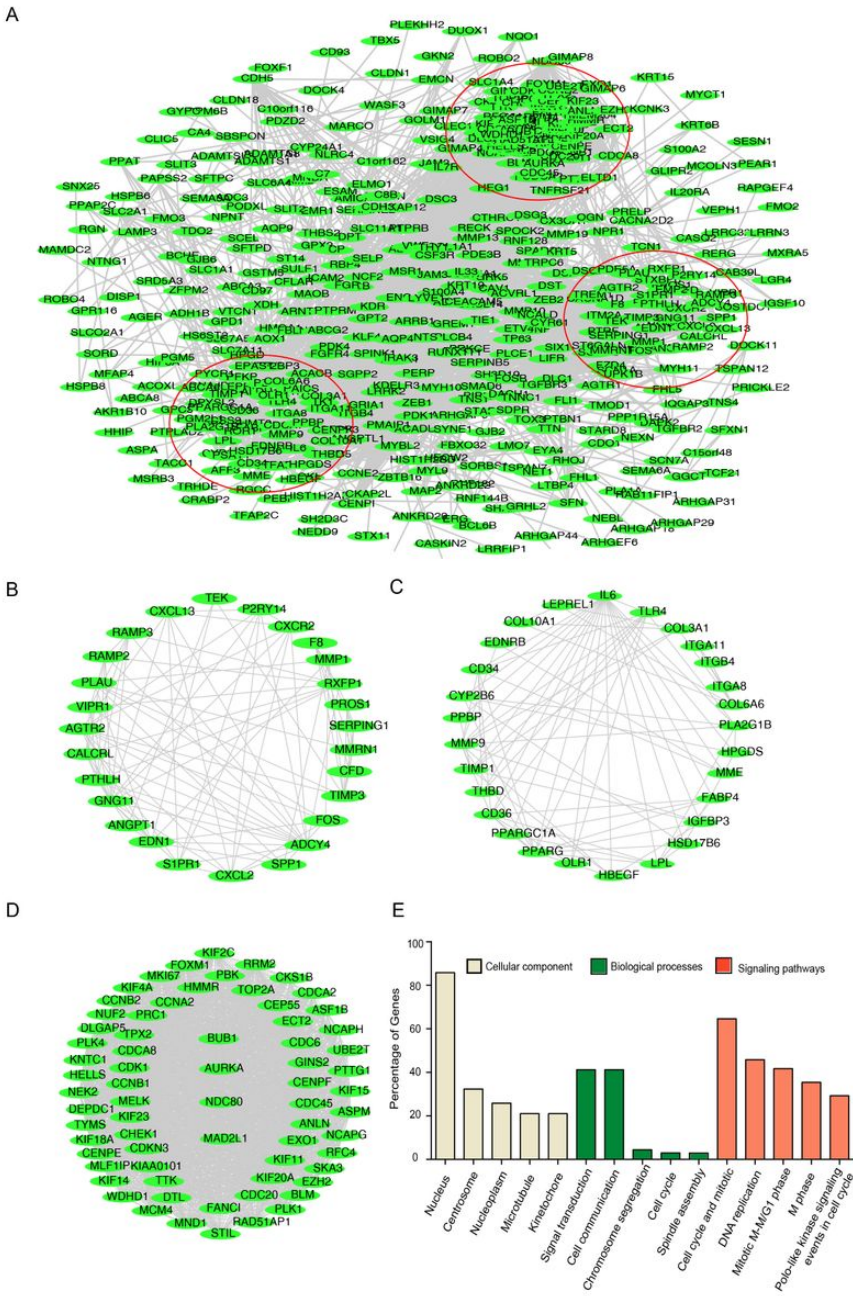


Figure 3

GDEs gene function modules analysis based on PPI network. (A) The PPI network of 664 GDEs, and three top gene modules analyzed based on the network, each red circle represents one gene module. (B-D) Three gene modules containing (B) 27, (C) 28 and (D) 69 GDEs respectively. (E) GO and KEGG analysis reveal the basis functions including cellular components, biological processes and signaling pathways the 69 genes in top module mainly enriched in.

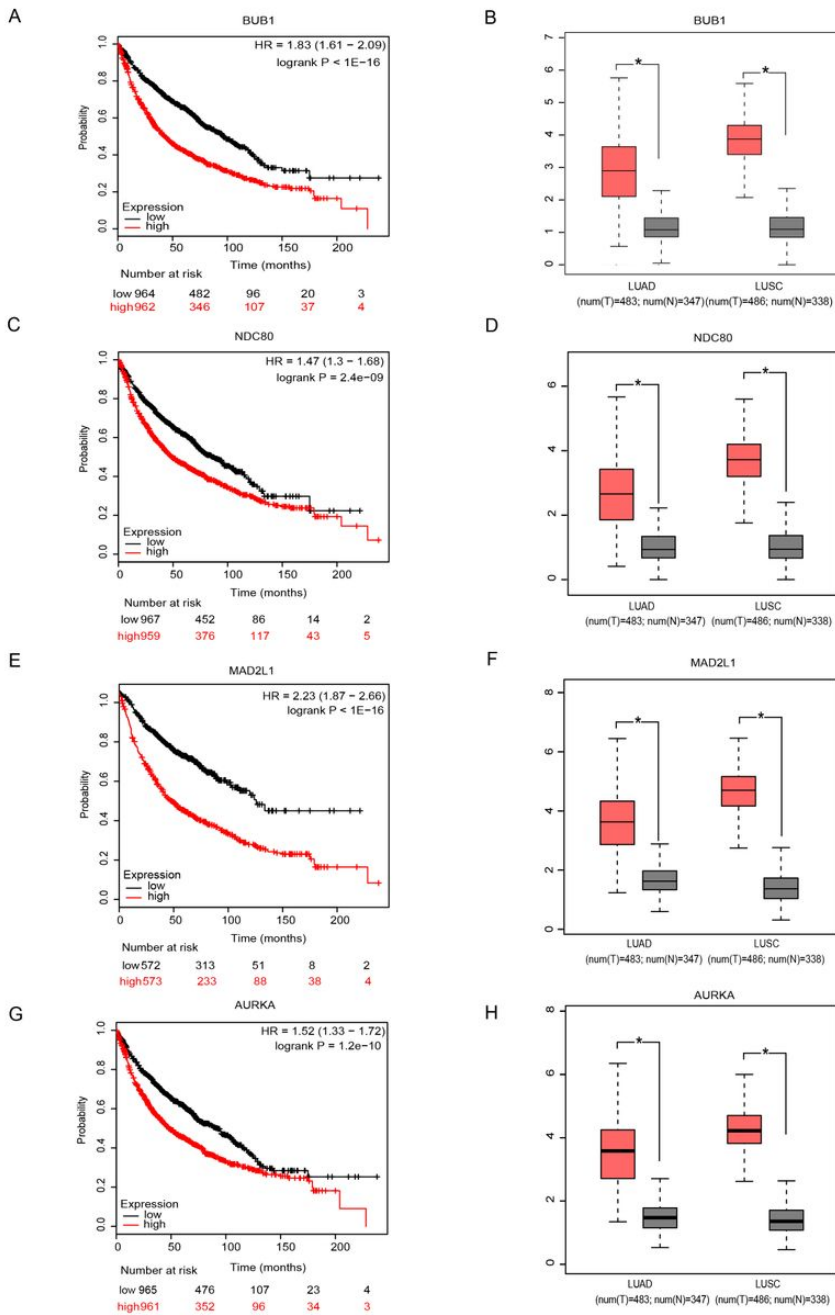


Figure 4

Os prognosis and expression information of 4 spindle assembly checkpoints genes. Overall survival value of (A) BUB1, (C) NDC80, (E) MAD2L1 and (G) AURKA in NSCLC; Expression level of (B) BUB1, (D) NDC80, (F) MAD2L1 and (H) AURKA in NSCLC cancer versus normal lung tissues, including adenocarcinoma (left column) squamous cancer (right column). * P<0.05.

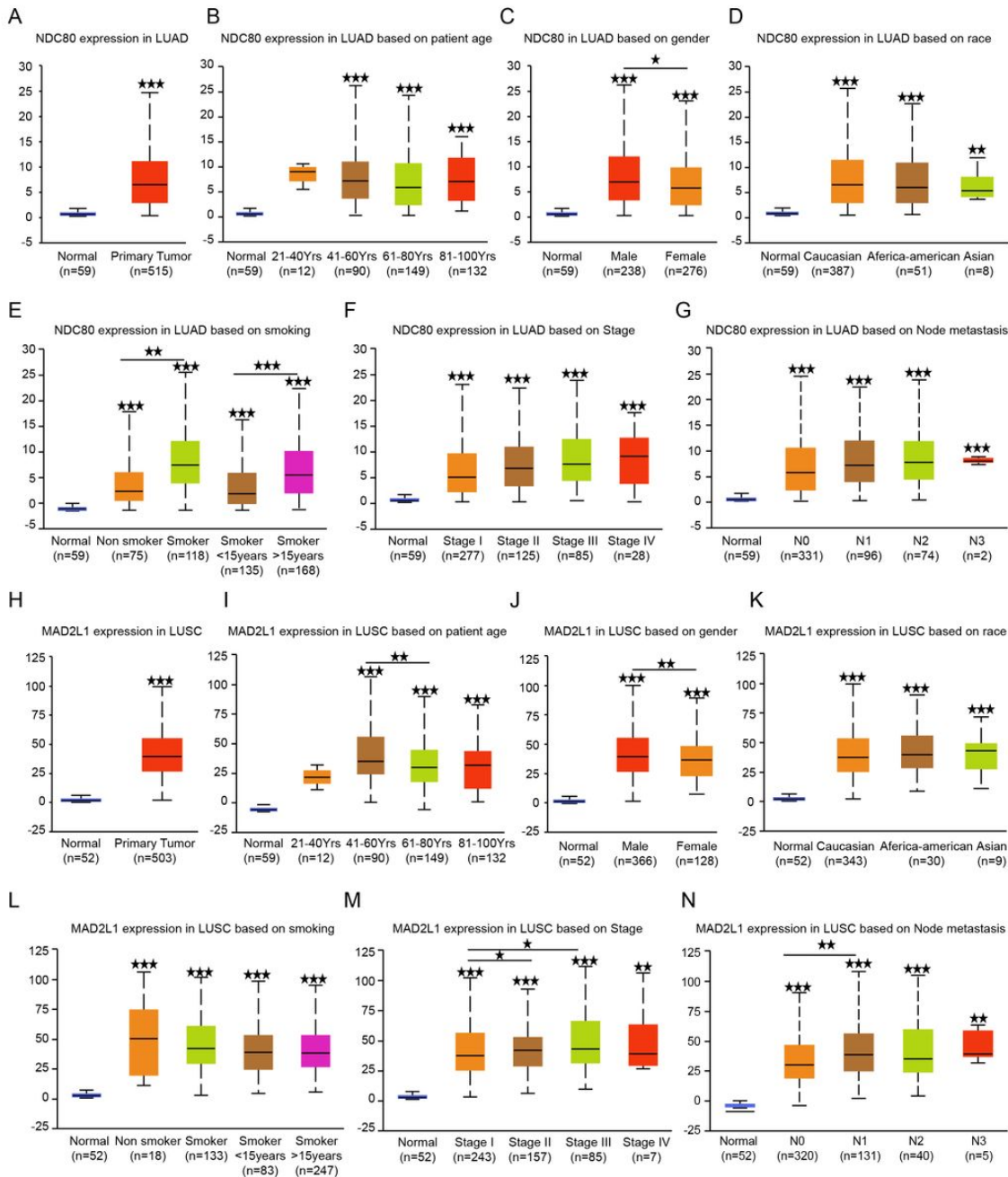


Figure 5

The relationship between NDC80, MAD2L1 expression and LUAD, LUSC clinical parameters (A) Relative NDC80 expression in LUAD. And the association between NDC80 expression and adenocarcinoma (B) patients age, (C) gender, (D) race, (E) smoking status, (F) tumor stage and (G) lymph node metastasis. (H) Relative MAD2L1 expression in lung squamous cell carcinoma. And the association between MAD2L1 expression and squamous cell carcinoma (I) patients age, (J) gender, (K) race, (L) smoking status, (M) tumor stage and (N) lymph node metastasis. * $p < 0.05$, ** $p < 0.01$, *** $p < 0.001$. (The first layer * which is right above the error bar representing comparison to normal group, and the above layers * which were above a secondary line represent the comparison between corresponding groups that were covered by the line)

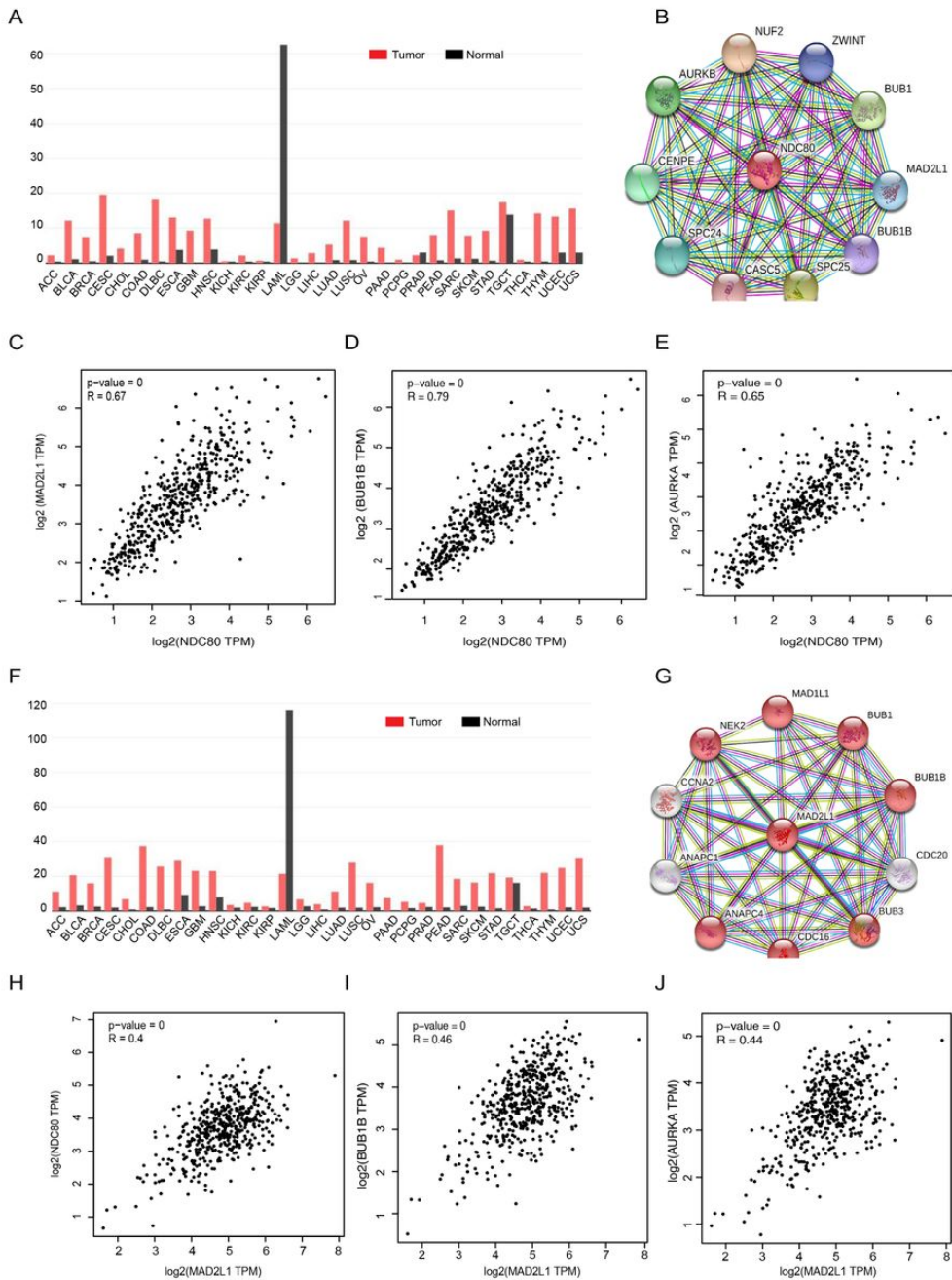


Figure 6

NDC80 and MAD2L1 related signaling analysis (A) Expression of NDC80 in various human cancers revealed by GEPIA. (B) NDC80 centered PPI network representing the genes most related to NDC80. (C-E) Correlation between NDC80 and (C) MAD2L1, (D) BUB1B and (E) AURKA in LUAD revealed by GEPIA ($R=0.67$, 0.79 , 0.65 respectively). (F) Expression of MAD2L1 in various human cancers revealed by GEPIA. (G) MAD2L1 centered PPI network representing the genes most related to MAD2L1. (H-J) Correlation between MAD2L1 and (H) NDC80, (I) BUB1B and (J) AURKA in LUSC revealed by GEPIA ($R=0.40$, 0.46 , 0.44 respectively).